DOI:10.1021/jf9018504

JOURNAL OF AGRICULTURAL AND FOOD CHEMISTRY
ARTICLE

Differentiation of Dried Sea Cucumber Products from Different Geographical Areas by Surface Desorption Atmospheric Pressure Chemical Ionization Mass Spectrometry

Zhongchen Wu,[†,‡] Huanwen Chen,*[,†] Weiling Wang,[⊥] Bin Jia,[†,‡] Tianlin Yang,[‡] Zhanfeng Zhao,[§] Jianhua Ding,[†] and Xuxian Xiao*[,⊥]

[†]Department of Applied Chemistry, East China Institute of Technology, Fuzhou 344000, People's Republic of China, [‡]School of Space Science and Physics, Shandong University at Weihai, Weihai 264209, People's Republic of China, [§]College of Information Science and Engineering, Harbin Institute of Technology at Weihai, Weihai 264209, People's Republic of China, and [⊥]School of Chemistry and Chemical Engineering, Central South University, Changsha 410083, People's Republic of China

Without any sample pretreatment, mass spectral fingerprints of 486 dried sea cucumber slices were rapidly recorded in the mass range of *m*/*z* 50−800 by using surface desorption atmospheric pressure chemical ionization mass spectrometry (DAPCI-MS). A set of 162 individual sea cucumbers (*Apostichopus japonicus* Selenka) grown up in 3 different geographical regions (Weihai: 59 individuals, 177 slices; Yantai: 53 individuals, 159 slices; Dalian: 50 individuals, 150 slices;) in north China sea were successfully differentiated according to their habitats both by Principal Components Analysis (PCA) and Soft Independent Modeling of Class Analogy (SIMCA) of the mass spectral raw data, demonstrating that DAPCI-MS is a practically convenient tool for high-throughput differentiation of sea cucumber products. It has been found that the difference between the body wall tissue and the epidermal tissue is heavily dependent on the habitats. The experimental data also show that the roughness of the sample surface contributes to the variance of the signal levels in a certain extent, but such variance does not fail the differentiation of the dried sea cucumber samples.

KEYWORDS: Surface desorption atmospheric pressure chemical ionization; sea cucumber; food analysis; surface analysis; mass spectrometry; principal component analysis; soft independent modeling of class analogy

INTRODUCTION

As a natural resource of nutrition and medicine, sea cucumber, a worm-shaped animal with an elongated body and leathery skin, has been widely consumed for centuries. Being served as one of the favorite sea foods and restorative medicine, sea cucumber is one of the important cultured aquatic species in China and many other Asian countries. Currently, there are about 1100 varieties of sea cucumbers in the world, and only 40 species are commercially or potentially important to human beings. In China, 134 species have been found, among which only about 20 species are edible (*1*).

For convenient storage and transportation, dried sea cucumbers are the most popular final products on markets. Dried sea cucumbers are promptly made after the fresh sea cucumbers are collected from the sea. After preliminary hand picking, the internal organs of qualified sea cucumbers are instantly removed, and then the nutrient body flesh is properly cleaned and then boiled while stirred in fresh water for 10 min to 1.5 h, depending on their body weight and sizes. After boiling, all the sea cucumbers are cooled down and dried in the air. The whole process may take 1−3 weeks to prepare well-qualified dried sea cucumber products. Many factors may influence the quality of products during the preparation process. For example, rehydrated sea cucumber samples have lower levels of total phenolics, free amino acid, docosahexaenoic acid (DHA), and ash, but significantly higher protein and fat contents than their fresh counterparts (*2*). Previous studies showed that the nutritional values of main constituents were changed in the treated or untreated sea product samples (*3*). However, nowadays dried sea cucumber products are made with regular work flows in northern China (*4*), and the unified processing criterions may have the same degree of influence on the products. It is also well-known that sea cucumbers of the same species but in different geological regions provide discriminative functions in medical applications (*5*, *6*) and, thus, require special treatments in commercial trade and safety management.

However, it is extremely difficult for ordinary consumers to distinguish sea cucumber products using sensory methods (e.g., by eyes, smell, taste, etc.), particularly when the products are pulverized as powder or cut into slices. The morphologic characteristics (body length, main color, tentacles, throat calcareous

*To whom correspondence should be addressed. Tel.: (+)86-794-8258703 (H.C.); 0086-13975199408 (X.X.). Fax: (+)86-794-8258320 (H.C.). E-mail: chw8868@gmail.com (H.C.); csuxywjhx@yahoo.com.cn (X.X.).

 Published on Web 09/29/2009 © 2009 American Chemical Society

ring, ossicles of the body wall, etc.) (*7*, *8*) and the structure of the carbohydrate chains of triterpene glycosides (*9*−*11*) have been used to resolve taxonomic problems in the classification of sea cucumbers. These methods require tedious sample pretreatments and multiple instrumental techniques but give no information about habitat information of samples. For plant tissue products, such as some Chinese herb medicines, the geographical regions were distinguishable using Fourier transform infrared (FT-IR) spectroscopy (*12*−*14*). Unfortunately, this method gave little information about the constituent and content characters and resulted in difficulty to differentiate sea cucumber products when it was applied to test our samples. Mass spectrometry such as isotope ratio mass spectrometry (IRMS) (*15*, *16*), gas chromatography mass spectrometry (GC-MS) (*17*, *18*), inductively coupled plasma mass spectrometry (ICP-MS) (*19*, *20*), and proton transfer reaction mass spectrometry (PTR-MS) (*21*) was used for assigning the regional origins of other agricultural products and food products. Generally, as reported elsewhere (*22*), these methods lack high throughput. For example, IRMS and GC-MS require time-consuming sample pretreatments; besides the multiple-step sample workup, ICP-MS works using a high-temperature argon plasma as the ionization source and thus detects only metallic or inorganic elements; PTR-MS is believed to be a one-dimensional technique (*23*), which provides limited information for analysis of sea cucumber products. Therefore, the development of novel methods for rapid classification of sea food products in various habitats is an urgent practical need.

Ambient mass spectrometric techniques (*24*−*34*) provide rapid analysis of complex samples with minimal sample pretreatments. Surface desorption atmospheric pressure chemical ionization mass spectrometry (DAPCI-MS) (*27*, *35*, *36*) has been successfully applied to online analysis of food samples (*37*−*39*) without neither sample pretreatment nor chemical contamination, and thus, it is of particular interest to monitor dried sea cucumber samples for rapid differentiation. In this report, a new method based on DAPCI-MS was established to rapidly differentiate various sea cucumber products of different geographical regions by PCA (*40*) and SIMCA (*41*) using the DAPCI-MS mass spectral fingerprints, which were directly recorded from the dried sea cucumber samples without any sample pretreatment. Our data showed that, under the positive ion detection mode, DAPCI-MS can simultaneously detect more than 52 major components from dried sea cucumber tissues, providing a convenient and fast method for rapid classification of sea food products.

MATERIALS AND METHODS

Dried sea cucumber samples in total of 162 individuals were randomly picked up from a local sea cucumber outlet. All the samples were cultured in three habitats (Weihai, habitat 01; Yantai, habitat 02; and Dalian, habitat 03) in the north China sea and identified as one species, *Apostichopus japonicus* (Holothuroidea, Stichopodidae), by Prof. Yu-lin LIAO (Marine Biological Museum, Chinese Academy of Sciences, Qingdao, China) according to the morphological characteristics of the dorsal ossicles (*7*). Dried sea cucumber samples were used as received. Every individual was uniformly cross cut to make three thin slices (1 mm thickness). Consequently, a total of 486 slices from three habitats such as Weihai (59 individuals, 177 slices), Yantai (53 individuals, 159 slices), and Dalian (50 individuals, 150 slices) were obtained for DAPCI-MS investigation.

Some slices are shown in **Figure 1** together with sea cucumber individual samples. Although different morphological features (e.g., body color, size, and the number of tentacles) are observed, these individuals belong to one species by professional identification. The moisture content of samples was not analyzed because

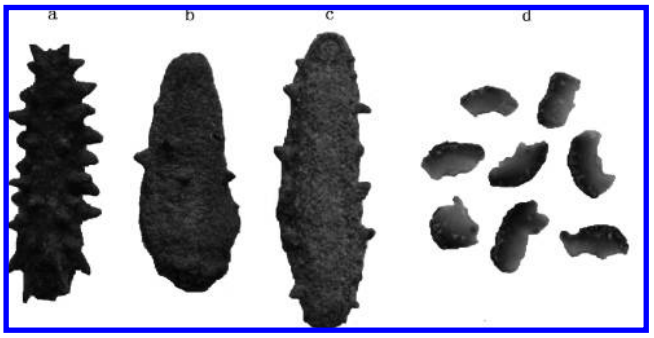

Figure 1. The sea cucumber (*Apostichopus japonicus*) samples from three habitats and their slices: (a) Weihai; (b) Yantai; (c) Dalian; (d) slices made from individuals matured in different habitats, showing no difference detectable by sensory methods.

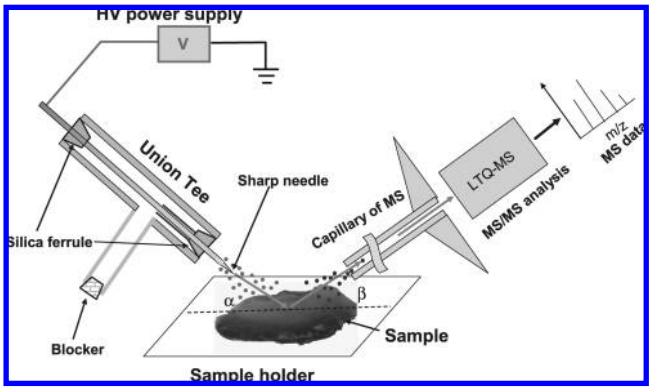

Figure 2. Schematic diagram of the DAPCI-MS for sea cucumber product analysis.

the samples were dried on the same degree, and the slight difference in the moisture would not seriously effect the results. The samples (slices) were used immediately for direct mass spectrometric analysis using the DAPCI without any further sample treatment. Each slice was measured 3−5 times to obtain the averaged results.

All the experiments were carried out using a commercial linear ion trap mass spectrometer (LTQ-XL, Finnigan, San Jose, CA) installed with a homemade surface desorption chemical ionization source. A cylindrical electrode (stainless steel, 5 cm in length and 0.2 mm in diameter), with a cone on one end (ca. 20 μm in diameter at the tip) and an insulator on the other end, was inserted into a fused-silica capillary (0.5 mm i.d.). The capillary and the sharp needle were coaxially fixed to a union tee (Swagelok, OH) using a silica ferrule and were carefully arranged such that about 0.5 mm of the sharp needle was exposed to air. The DAPCI source was operated in a gasless mode; thus, no sheath gas was required. Ambient air about 65% relative water moisture was used as a reagent for chemical ionization in this study. The temperature of the heated capillary of the LTQ was maintained at 150 °C. The distance between the discharge tip and the MS inlet was 5−10 mm (depending on the size of the samples), and the distance between the discharge tip and sea cucumber slices was about 2 mm (schematically shown in **Figure 2**). The sampling area was about 3 mm^2. A high voltage (+4 kV, discharge current 1−2 mA) was applied to the sharp needle of surface desorption chemical ionization source. The LTQ-MS instrument was set to work in a positive ion detection mode, and the incident angle and the reflecting angle were set at 30°. The default values of voltages for the tube lenses, conversion dynode, detectors were directly used. No further optimization was performed.

Under the working conditions, mass spectral fingerprints of 486 slices were directly recorded using DAPCI-MS in the mass range of m/z 50−800 Da once the sample slice was loaded. All the

mass spectra were background subtracted using the Xcalibur software of the LTQ instrument. The raw data were automatically saved as RAW files. As a standard feature of the LTQ-MS instrument, the mass spectra were then exported to the clipboard as text files and then exported to an Excel software. To ensure the accuracy of the data conversion, each m/z unit (e.g., m/z 80−81) was sampled by 11 points. All text data were arranged using the m/z values as independent variables and the absolute signal intensities of the full scan mass fingerprint (MS^1; 8250 data points in total) rather than collision-induced dissociation (CID) spectra as dependent variables. The whole mass spectral data, including all of characteristic peaks (such as m/z 74, 102, 130, 158, and 315), were treated as a matrix, $X(p \times n)$, in which the rows and the columns corresponded to p samples ($p = 486$) and n m/z value variables ($n = 8250$). The mass fingerprint data recorded from the slices derived from the same sea cucumber individual were adjacently listed in three rows in the matrix $X(p \times n)$, which were mathematically averaged according to the formula below to overcome the chemical heterogeneity of the slices obtained from the same individual sea cucumber sample.

$$X_{j,n}^{\text{mean}} = \frac{X_{3j-2,n}+X_{3j-1,n}+X_{3j,n}}{3} \quad \{X_{j,n}|j = 1, \ldots, 162, n = 1, \ldots, 8250\} \tag{1}$$

where j was the number of individual sea cucumber products. Averaging of data has the same effect as the homogenization of the samples. To homogenize the data of peak intensities, especially those of the peaks with relatively high intensities, another data-pretreatment method, autoscaling, was performed using the "auto" function by using "PLS_Toolbox 2.1" (for use with Matlab, eigenvector Research, Inc., Manson, WA). In this case, all the variables (columns) of the matrix X_n^{mean} were transformed according to

$$X_{j,n}^{\text{autoscaled}} = \frac{X_{j,n}^{\text{mean}} - \overline{X}_n^{\text{mean}}}{S(X_n^{\text{mean}})} \tag{2}$$

where $\overline{X}_n^{\text{mean}}$ and $S(X_n^{\text{mean}})$ were the mean and the standard deviation (S.D.), respectively, for each column of the matrix $X^{\text{mean}}{}_{j,n}$.

The autoscaled data matrix ($X_{j,n}^{\text{autoscaled}}$) were finally imported to the STATISTICA (version 6.0, StatSoft Inc., Tulsa, U.S.A.) spreadsheets (.sta files) and "PLS_Toolbox 2.1" for PCA and SIMCA analysis, respectively. Once the data were loaded successfully into the above two software programs, they were used directly for PCA and SIMCA processing without any further data treatment. When the calculation of PCA was finished, only the loadings and scores of the first three principal components (PCs) were respectively exported to new spreadsheets, because the first three PCs captured most of the variances in the data set. Matlab (version 7.1, Mathworks Inc., Natick, U.S.A.) software was utilized to present the results of statistical analysis for better visualization.

To acquire CID mass spectra, 20−35% collision energy (arbitrary units defined by the LTQ instrument) was applied to excite the isolated precursor ions of interest using a mass window of 1 mass/charge unit. A typical duration for the CID experiment was 30 ms.

RESULTS AND DISCUSSION

Representative Mass Spectral Fingerprints. When the positive high voltage (+4 kV) was applied to the sharp needle of the surface desorption chemical ionization source in the air with high water moisture (*36*), the water molecules in the air were ionized to generate the primary ions (H_3O^+), which were accelerated by the electric field to bombard the surface of samples. The analytes on the sea cucumber slices were ionized, and analyte ions were introduced through the ion guide system of the LTQ instrument into the analyzer for further mass analysis and structure identification.

The mass spectral fingerprint was averaged with 36 scans, which took 12 s in total (shown in Figure S1 in the Supporting Information). Without tedious sample pretreatment, the only time-consuming steps of the experimental procedure are the section preparation and sample loading, which take about 2 min for a single run. Sea cucumbers are alternatively supplied as slices on the market, thus, the section preparation is not a need in such a case. The sample loading is manually done, which consumes about 30 s per loading. The analysis speed can be further improved by using an autosample introduction system (*26*). Thus, DAPCI-MS provides advantages for high throughput and online analysis of sea food products.

More than 52 compounds were detected from all the samples, showing multiple peaks with significant signal intensities in the mass range of 50−800 Da. Among all the mass spectral fingerprints, the protonated molecules detected at m/z 158, 136, 130, 74, and 102 dominated all the mass spectra recorded from the body wall tissue with relatively high intensities (4.08×10^6, 1.33×10^6, 9.8×10^5, 3.8×10^5, and 1.9×10^5 cps, respectively). The remarkably high intensities were probably ascribed to the high concentration of the analytes and the relatively high gas phase basicities of the analytes. Meanwhile, there were numerous peaks detected with relatively low intensities (about 1.0×10^4 cps) in the mass spectral fingerprints. These peaks were clearly visible with good signal-to-noise ratios (S/N, 100:1) in the zoomed views of the spectra (**Figure 3**). The data showed the good response of DAPCI for a wide dynamic range of analytes. The peak at m/z 158 was not zoomed because it was the most abundant peak in all the mass spectral fingerprints. The rest of peaks, after amplification by different times, were clearly shown in all the mass spectra. As shown in **Figure 3**, fewer peaks were detected in the mass range over m/z 600. This is because those large biological molecules have higher affinities to the biological tissue (i.e., the sea cucumber slice) than the small molecules. Furthermore, the mass spectral fingerprints of three different geographical regions showed no essential differences in terms of m/z value and peak density, probably because all of the sea cucumber samples belong to the same species and thus should have very similar molecular profiles.

Epidermis, the largest tissue of sea cucumber, was also investigated, under the same experimental conditions as those for the body wall tissue experiments, using intact individual samples instead of slices. For the samples collected from the same habitat, the mass spectral fingerprints recorded from the epidermis tissue (Figure S2 in the Supporting Information) are very similar to those spectra recorded from the body wall tissues. No significant differences were observed in terms of mass-to-charge ratio, signal-to-noise ratio, and relative peak intensity. These findings suggested that the detectable chemicals of the sea cucumber could be distributed through the whole body, except for the difference in concentrations. This suggests that the epidermis tissue is as important as the body wall in views of components. Therefore, the epidermis tissue should be well used during the sea cucumber production and manufacturing process.

As noted in previous studies (*37*), the signal levels vary in DAPCI-MS, especially for direct analysis of rough surfaces. As shown in **Figure 1**, the skin surface of an intact sea cucumber presents bumpy features, and even the well cut slices are of coarse edges. Thus, it is not surprising to see the signal of DAPCI-MS fluctuates in a reasonably wide range. On the other hand, it's worth noting that the sampling area of DAPCI-MS was less than 10 mm^2. In such a small area, the effect caused by the bumpy features may be not as severe as what we have seen in the **Figure 1**.

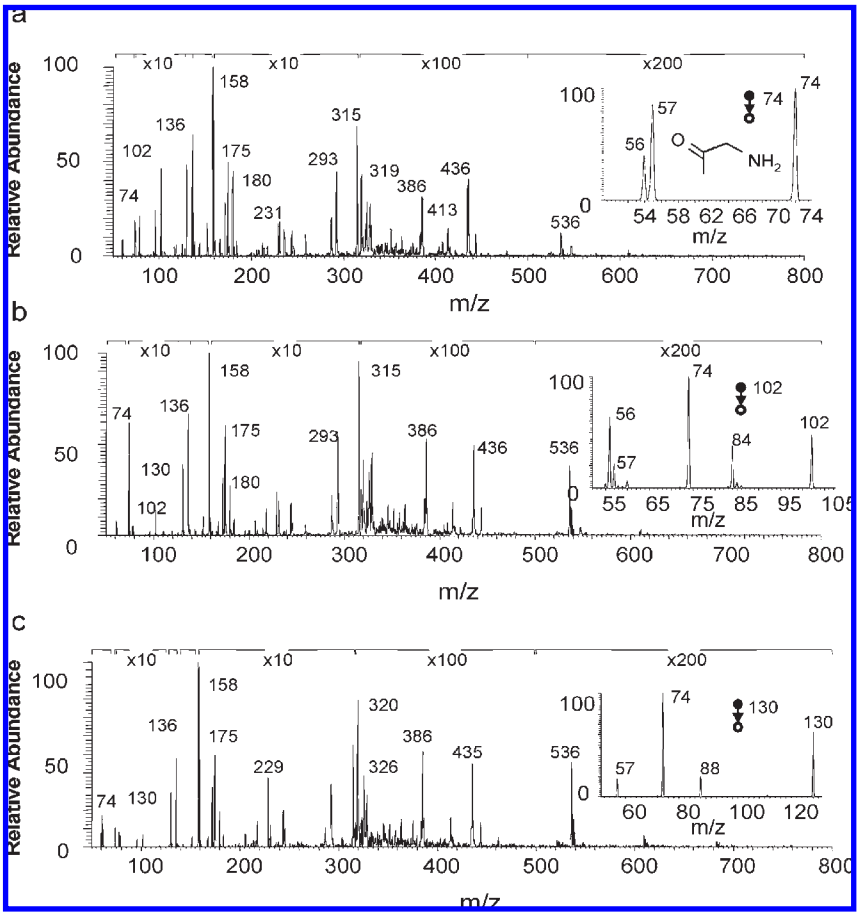

Figure 3. Representative mass fingerprints of body wall of three different geographical origins and CID spectra of interest. The product ion (*m*/*z* 74) was tentatively assigned based on the MS/MS spectral data: (a) Weihai; (b) Yantai; (c) Dalian.

Although the rough surfaces have affected on the distribution of signals in a certain level, the epidermis tissue is unable to be easily prepared because it is very thin. The epidermis tissue is maintained in the native conditions of the dried sea cucumber samples, showing the capability of DAPCI for the characterization of complex surfaces.

The statistic analysis results obtained using STATISTICA 6.0 showed the distribution characteristics of some predominant signals observed in the mass spectral fingerprints (as shown in **Figure 4**). Clearly, the peak intensities of a given peak (e.g., *m*/*z* 158, 136) are variable in a certain degree (±10−28%) in both mass spectra recorded from either the body wall samples or the epidermis tissues. For a given peak (e.g., *m*/*z* 158), the signal dispersion found in the epidermis tissue samples is relatively more significant (alteration max. 25%) than that found in the body wall samples (alteration max. 14%). This is probably because the epidermis affects the signal level more seriously than that of the body wall tissue. Actually, the roughness of the body wall tissue (slice) is much lower than that of the epidermis tissue (as shown in **Figure 1**). For a given sample, the deviation of the signal was less than 5% of the mean value in most measurements. Thus, the deviation of the signal recorded from different individuals is most attributed to the individual difference of certain chemical component distributed in the different samples. Some of the chemicals were detected at very small variation signal levels (e.g., *m*/*z* 74, 102, and 315) in both the body wall tissue and the epidermis tissue, showing that these compounds were possibly more evenly distributed in these samples. The information about the signals detected from samples of different habitats is also visualized in **Figure 4**. For example, the signal intensities of the peaks at *m*/*z* 130 and *m*/*z* 136 differentiate the sample geographical regions, and the variances of the two peaks between the habitat 01 and habitat 03 are much larger than others. This suggests that the compounds may distribute at quite different levels in the sea cucumber samples grown up in various geological regions, which has been observed in natural plant products (*42*). It is also reasonable to be seen in animal products such as sea cucumbers since growth conditions such as food, water depth, water quality, and oxygen exposure are usually various in different habitats (*43*). On the other hand, **Figure 4** shows that the differential peak intensity of single peak is not enough to separate the samples according to their geographical regions because the signal overlap commonly exists among the different habitat samples. Thus, methods that cannot generate chemical fingerprints are difficult for rapidly differentiating the geographical region of samples. This makes DAPCI-MS very useful for fast classification of sea cucumbers according to their habitats based on the mass spectral fingerprints.

To picture the difference between given signals of two kinds of tissues (body wall and epidermis) detected from different samples, comparative analysis was done using their averaged spectral intensities (the middle bar between the upper boundary and lower boundary in the **Figure 4**). The comparison diagram was shown in the **Figure 5**. Except for the peak of habitat 01 at *m*/*z* 158, the mass spectral signal intensities of the body wall samples are much stronger than those of epidermis tissue samples for all of samples from the three different habitats. Meanwhile, the peak absolute intensity of samples (both body wall and epidermis tissue) from habitat 01 (**Figure 5**a) was the strongest, and that from habitat 03 (**Figure 5**c) was the weakest among the three different habitats.

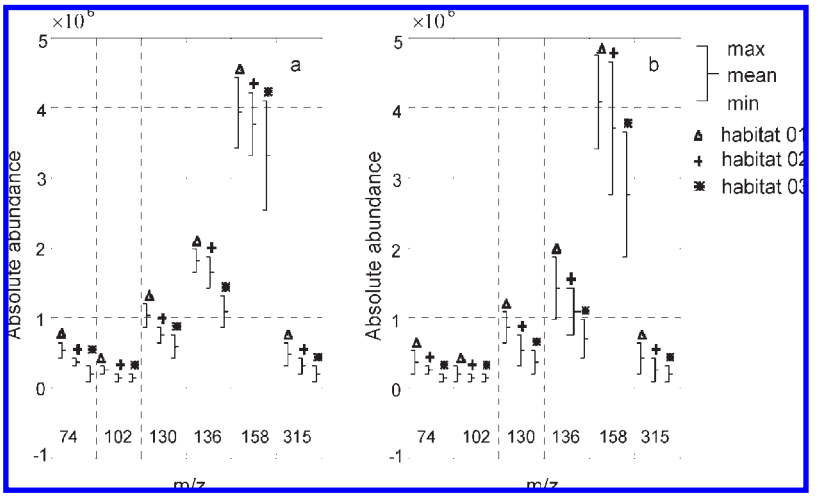

Figure 4. Range plots representing the absolute intensity distribution of typical mass spectral peaks of body wall and epidermis tissue. The mean value is shown by the middle bar. The upper/lower boundary indicates the maximal/minimum value. The habitat 1 is Weihai, the habitat 2 is Yantai, and the habitate 3 is Dalian: (a) the distribution of body wall data and (b) the distribution of epidermis tissue data.

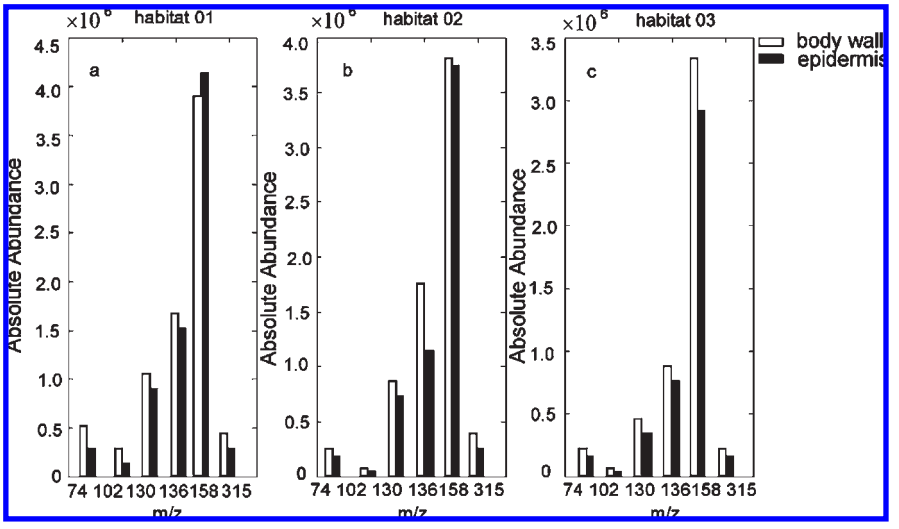

Figure 5. Stick diagrams of the typical peak intensity of body wall and epidermis tissue samples from various habitats: (a) Weihai; (b) Yantai; (c) Dalian.

The distribution of constituent contents of sea cucumber shows significant difference among the groups and different tissues, which have also been reported by other papers (*2*). For the typical peaks, the correlation coefficients (*44*) (standard covariance) of the data generated using two tissues samples were 0.994 (habitat 01), 0.997 (habitat 02), and 0.999 (habitat 03), respectively. As we know, the value of the correlation coefficient stands for the similarity degree of spectral data. So, the results support that the body wall tissues and the epidermis tissues of habitat 01 have the most significant difference in peak intensity.

Representative CID Mass Spectra. Theoretically, molecules detected can be identified using multiple-stage tandem mass spectrometry experiments. As a demonstration, only signals of interest were tentatively identified in this study. For example, the peak at *m*/*z* 74, with mediate relative intensity, generated major fragments of *m*/*z* 56 and 57 by the loss of H_2O and NH_3, respectively, under the mild CID conditions (20% CE, 30 ms). Under such mild conditions, the cleavage of OH radical is generally disfavored since radical generation usually involves energetic processes (*45*, *46*). Thus, the observation of the neutral loss of NH_3 suggested the precursor ions contained $-NH_2$ group. The relatively high intensity of the peak at *m*/*z* 74 also indicated that the molecule included basic groups such as $-NH_2$. As shown in the inset of **Figure 3**a, the abundance of the peak at *m*/*z* 57 is much higher than that of the peak at *m*/*z* 56. This reveals useful information about the molecular structure, indicating the molecule contains no free −OH group. Therefore, the molecular structure of the signal detected was illustrated as the scheme shown in the inset of **Figure 3**a. A similar fragmentation pattern was also obtained using the authentic compound of aminoacetone, which plays important roles in metabolism (*47*−*51*). This indicates that the DAPCI-MS method is powerful to investigate the metabolic process and other important life processes. Similarly, other peaks such as *m*/*z* 102 and 130 were tentatively assigned to be compounds containing $-NH_2$ and −OH. In the CID spectrum of *m*/*z* 102, the main fragments of *m*/*z* 84 and 74 were derived from the precursor ion by the loss of 18 and 28 mass units, corresponding to H_2O and CO, respectively. The fragments of *m*/*z* 74 further generated two fragments of *m*/*z* 56 and 57 by the loss of H_2O and NH_3, which were shown in the MS^3 spectrum of the ions of *m*/*z* 74 and shown in the MS^2 spectrum of ions of *m*/*z* 102 (shown in the inset of **Figure 3**b). Similarly, the precursor ions of *m*/*z* 130 formed fragments of *m*/*z* 88 and 74 by lose of CH_2CO and C_3H_4O. Further experiments showed that the fragment of *m*/*z* 74 dissociated as same manner as

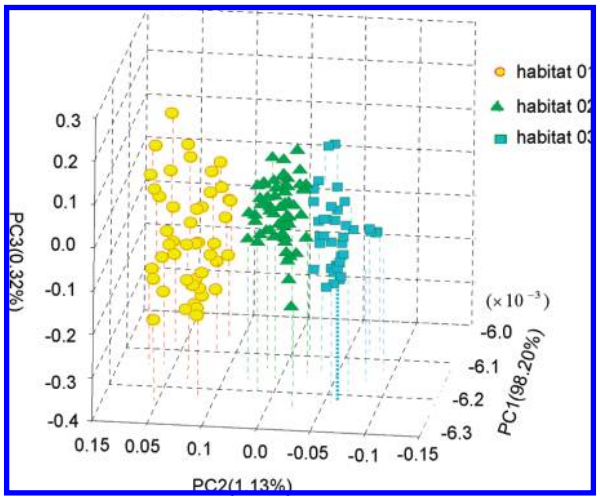

Figure 6. 3D plots of PCA score results for 162 sea cucumber samples (The habitat 1 is Weihai; the habitat 2 is Yantai; and the habitat 3 is Dalian). The data points of the same habitat were marked with the same symbols.

that of *m*/*z* 102. It was unlikely to form clusters such as $N_2 + M$ in DAPCI-MS, and thus the signals detected suggested that the molecule (*m*/*z* 74) serves as a molecular block to build up molecules detected at *m*/*z* 102 and *m*/*z* 130. Note that numerous ionized molecules were successfully detected from the sea cucumber samples by DAPCI-MS. All of the peaks detected could be identified by multiple-stage tandem mass spectrometry, plus the use of reference compounds for improved confidence if necessary. However, it is beyond the scope of this work to interpret all of the detected peaks.

Principal Components Analysis of Mass Spectral Signals. As a popular multiple variance statistical tool, PCA was employed to classify the samples. **Figure 6** showed the PCA results obtained using the autoscaled data of DAPCI-MS spectral matrix ($X_{j,n}^{\text{autoscaled}}$). The first three PCs were selected for modeling, because the percentages of variance explained by PC1 (eigenvalue, 159.14), PC2 (eigenvalue, 1.83), and PC3 (eigenvalue, 0.53) were 98.20, 1.13, and 0.32%, respectively. Thus, those PCs represented about 99.65% of the total variance. The first PC described the direction of the greatest variation (i.e., the variation of the peak intensities) in the data set. Confident differentiation of samples according to their habitats has been achieved (shown in **Figure 6**), in which the cluster of habitat 01 was located much farther to habitat 03. The results of cluster analysis were in agreement with the characters of mass fingerprint data (shown in **Figure 4**). Small numerical interval (from −0.006 to −0.0063) were noticed in the scores of PC1 (details shown in Figure S3 in the Supporting Information), confirming that no outlier samples existed. This indicated the good representation of samples. The PC2 had the best distinguishing capacity for the identification of the original habitats, which indicated it just rightly stood for difference of the habitats. In **Figure 6**, the variability in a PCA context of sea cucumber individuals from same habitat (marked by same symbol) and from other habitats was clearly shown. The samples from different habitats were strictly distinguished because all the data from same habitat distributed in a relatively concentrated area. The distribution proved the satisfying representation of every habitat. PCA was also performed using the mass spectral raw data of the epidermis tissue to differentiate habitats. The results are also acceptable for sea cucumber habitat identification. Meanwhile, our preliminary data showed that DAPCI-MS combined with PCA can be helpful to differentiate sea cucumber species, providing a useful method to prevent people from eating sea cucumber products of inedible species.

PCA is a powerful tool for data compression and information extraction. In this experiment, the majority of information was effectually extracted by this algorithm. The loadings are normally linear combinations of the pure component. The loading plots of the first three factors were shown in Figure S4 in the Supporting Information, with readily identifiable peaks due to several abundant mass spectral peaks (*m*/*z* 74, 102, 130, 136, 158, and 315), which were the most predominant peaks in mass spectral fingerprints (**Figure 3**). Those peaks have significant changes in terms of intensity, and could be used as major molecular markers to probe the original habitats of sea cucumber. These peaks present in a very narrow mass range in the mass spectra, indicating that the mass spectrum is not necessary for the classification. Similar separation was achieved using at least three of six differential molecular signals (such as *m*/*z* 74, 102, 130, or *m*/*z* 136, 158, 315) (shown in Figure S5 in the Supporting Information). The overlap of peak intensities recorded using different samples (seen in **Figure 4**) reduced the resolving power of the PCA algorithm. However, detecting of three discrete signals rather than scanning the whole mass spectrum simplifies the mass spectrometer instruments and the analysis process as well. This is consistent with previous studies, where tea products were classified using the DAPCI-MS data (*37*). This signifies that a cheap, simple mass spectrometer instead of large, expensive commercially available instruments can be used to achieve the same separation using these differential peaks. This is very important for the industry applications because a mass spectrometer covering a wide spectrum band is much more expensive than miniature instruments.

The differences between body wall tissue samples and epidermis tissue samples were also analyzed using PCA. **Figure 7** shows the PCA score plots obtained using all the samples of different geographical regions. For the samples coming from habitat 01, the body wall tissue samples were apparently separated from the epidermis tissue samples (**Figure 7**a). The corresponding loading plots were shown in Figure S6 in the Supporting Information. From the loading plots, it is found that the signal detected at *m*/*z* 158, 136, and 130 contributed most to differentiate the samples. For the samples from the other two habitats, serious overlaps were found in the PCA score plots (**Figure 7**b,c). The chemical constituents detected were the key factors contributing to the PCA score plots. The PCA results shown in **Figure 7**b,c suggested that there were no essential differences in the body wall tissue from the epidermis tissue of the sea cucumber samples collected from either Yantai or Dalian.

Soft Independent Modeling of Class Analogy Analysis of Mass Spectral Signals. SIMCA, a supervised pattern recognition method, was also employed to classify the sea cucumber samples using the autoscaled data ($X_{j,n}^{\text{autoscaled}}$). SIMCA models were developed for each of the three defined classes (i.e., three habitats). The whole autoscaled data set was split into the calibration set (even-numbered rows of the matrix $X_{j,n}^{\text{autoscaled}}$) and validation set (odd-numbered rows of the matrix $X_{j,n}^{\text{autoscaled}}$) to represent the whole sample sets without bias (*52*). For new objects (the validation set), the distance (i.e., the residual variance) to all defined classes (the calibration set) would be calculated following the strategy demonstrated previously (*53*). As shown in **Figure 8**, the results justify the use of **Q** statistics and $\mathbf{T}^2$ criteria in the present study, as few outliers were detected. Thus, **Figure 8** depicted the best calibration models for each class. The crossed green lines stood for the 95% confidence limits of $\mathbf{T}^2$ and **Q** statistic (both marked in the figure). Clearly, the classes were mainly separated by the distance (i.e., **Q**) of "foreign" objects to a class rather than by the

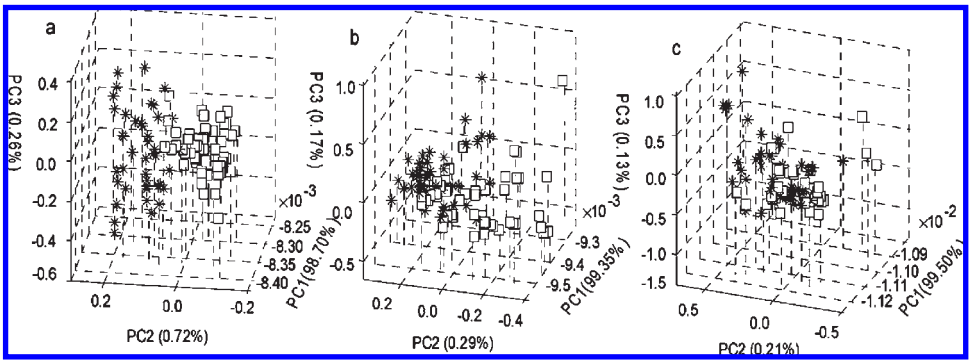

Figure 7. 3D plots of PCA score results for body wall and epidermis tissue mass spectrum data of the same origin: (a) samples collected from Weihai; (b) samples collected from Yantai; (c) samples collected from Dalian.

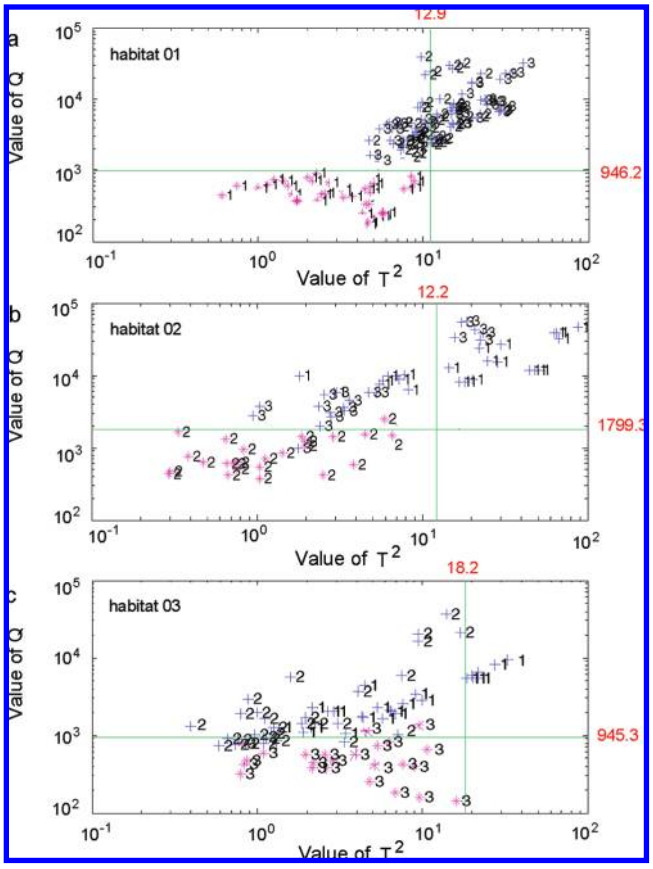

Figure 8. Calibration models for three classes of sea cucumber samples by SIMCA model using the calibration set data. The purple asterisk symbols denote members of a modeled class and the blue plus signs represent the members of the remaining two classes.

variation in their scores (i.e., $\mathbf{T}^2$), and only a few objects from one class fell into the space belonging to other classes (1 out of 26 for class 02; 2 out of 25 for class 03, 0 out of 30 for class 01; **Figure 8**c). After all three models had been developed on the calibration set, the new objects of validation set were classified by cross-validation using the above three defined models. As the result, high correction identification ratios (100% for habitat 01, selected 4PCs; about 97% for habitat 02, selected 4PCs; about 96% for habitat 03, selected 5PCs) were achieved. Therefore, SIMCA was also able to successfully differentiate the different geographical regions of sea cucumber samples, and validated the results obtained using PCA.

Our data showed that DAPCI-MS is a useful analytical tool for high throughput differentiation of sea cucumber products with different geographical regions, providing high sensitivity and high information content. By using water moisture (≥60% relative humidity) in the air as a reagent, DAPCI-MS provides simplicity and convenience for in situ analysis of food products at atmospheric pressure without toxic contamination. This makes DAPCI-MS a highly effective choice for high-throughput, real-time, and online analysis of biological samples with various complex matrices. Based on the DAPCI-MS data, the geographical regions of dried sea cucumber products are identified easily, although it cannot be accomplished using less than three mass spectral peaks. The peaks of interests in the mass fingerprints can be identified by multiple-stage tandem mass spectrometry. The distribution of detected molecular can also be investigated. These merits are particularly attractive for commercial trade and safety management, particularly in cases where unsatisfactory results are possibly generated by other methods such as morphologic characteristics analysis and sensory measurement.

On the other hand, the high cost of commercial mass spectrometers maybe prevents wide application of this method. This disadvantageous factor could be potentially solved by using miniature mass spectrometers with reduced size and cost, because differentially characteristic ions of the mass spectral data can be chosen as molecular markers to distinguish the species of sea cucumber.

ABBREVIATIONS USED

DAPCI-MS, surface desorption atomospheric pressure chemical ionization mass spectrometry; PCA, principal components analysis; SIMCA, soft independent modeling of class analogy; DHA, docosahexaenoic acid; FT-IR, Fourier transform infrared; IRMS, isotope ratio mass spectrometry; GC-MS, gas chromatography mass spectrometry; ICP-MS, inductively coupled plasma mass spectrometry; PTR-MS, proton transfer reaction mass spectrometry; CID, collision-induced dissociation; S.D., standard deviation; PCs, principal components; S/N, signal-to-noise ratios.

ACKNOWLEDGMENT

Authors own sincere thanks to Prof. Yu-lin LIAO (Marine Biological Museum, Chinese Academy of Sciences, Qingdao, China) for help identifying the species of sea cucumber products. This work is supported by the innovation method Fund of China (No. 2008IM040400).

Supporting Information Available: Figures supporting the experimental findings and discussions described in the main text. This material is available free of charge via the Internet at http://pubs.acs.org.

LITERATURE CITED

(1) Chen, J. X. Overview of sea cucumber farming and sea ranching practices in China. *SPC Beche-de-mer Inf. Bull.* **2003**, *18*, 18–23.

(2) Zhong, Y.; Khan, M. A.; Shahidi, F. Compositional characteristics and antioxidant properties of fresh and processed sea cucumber (*Cucumaria frondosa*). *J. Agric. Food Chem.* **2007**, *55*, 1188–1192.

(3) Cruz-Romero, M. C.; Kerry, J. P.; Kelly, A. L. Fatty acids, volatile compounds and colour changes in high-pressure-treated oysters (*Crassostrea gigas*). *Innovative Food Sci. Emergiing Technol.* **2008**, *9*, 54–61.

(4) http://www.fao.org/docrep/007/y5501e/y5501e08.htm.

(5) Wang, J. F.; Pang, L.; Wang, Y. M.; Gao, S.; Xue, C. H. Studies on the treatment effects of *Pearsonothuria graeffei* and *Apostichopus japonicus* on hyperlipidemia rats. *Period. Ocean Univ. China* **2007**, *337* (4), 597–600.

(6) Zhao, Q.; Wang, J. F.; Xue, Y.; Wang, Y.; Gao, S.; Lei, M.; Xue, C. H. Comparative study on the bioactive components and immune function of three species of sea cucumber. *J. Fish. Sci. Chin.* **2008**, *15* (1), 154–159.

(7) Li, Y.; Fei, L. H.; Chen, J. X. The morphology of ossicles of 15 commercial holothurians. *Period. Ocean Univ. China* **2008**, *32* (2), 211–216.

(8) Liao, Y. L. Sea cucumbers, holothurians from China. *Bull. Biol.* **2001**, *35* (9), 1–3.

(9) Moraes, G.; Norhcote, P. C.; Kalinin, V. I.; Avilov, S. A.; Silchenko, A. S.; Dmitrenok, P. S.; Stonik, V. A.; Levin, V. S. Structure of the major triterpene glycoside from the sea cucumber stichopus mollis and evidence to reclassify this species into the new genus australostichopus. *Biochem. Syst. Ecol.* **2004**, *32*, 637–650.

(10) Kalinin, V. I.; Silchenko, A. S.; Avilov, S. A.; Stonik, V. A.; Smirnov, A. V. Sea cucumbers triterpene glycosides, the recent progress in structural elucidation and chemotaxonomy. *Phytochem. Rev.* **2005**, *4*, 221–236.

(11) Avilov, S. A.; Kalinin, V. I.; Smirnov, A. V. Use of triterpene glycosides for resolving taxonomic problems in the sea cucumber genus Cucumaria (*Holothurioidea*, *Echinodermata*). *Biochem. Syst. Ecol.* **2004**, *32*, 715–733.

(12) Wang, L.; Lee, F. S. C.; Wang, X. R. Near-infrared spectroscopy for classification of licorice (*Glycyrrhizia uralensis* Fisch) and prediction of the glycyrrhizic acid (GA) content. *LWT—Food Sci. Technol.* **2007**, *40* (1), 83–88.

(13) Woo, Y. A.; Kim, H. J.; Cho, J.; Chung, H. Discrimination of herbal medicines according to geographical origin with near infrared reflectance spectroscopy and pattern recognition techniques. *J. Pharm. Biomed. Anal.* **1999**, *21*, 407–413.

(14) Li, Y. M.; Sun, S. Q.; Zhou, Q.; Qin, Z.; Tao, J. X.; Wang, J.; Fang, X. Identification of American ginseng from different regions using FT-IR and two-dimensional correlation IR spectroscopy. *Vib. Spectrosc.* **2004**, *36*, 227–232.

(15) Renou, J. P.; Bielicki, G.; Deponge, C.; Gachon, P.; Micol, D.; Ritz, P. Characterization of animal products according to geographic origin and feeding diet using nuclear magnetic resonance and isotope ratio mass spectrometry. Part II: beef meat. *Food Chem.* **2004**, *86*, 251–256.

(16) Georgi, M.; Voerkelius, S.; Rossmann, A.; Grassmann, J.; Schnitzler, W. H. Multielement isotope ratios of vegetables from integrated and organic production. *Plant Soil* **2005**, *275*, 93–100.

(17) Fernandez, C.; Astier, C.; Rock, E.; Coulon, J. B.; Berdague, J. L. Characterisation of milk by analysis of its terpene fractions. *Int. J. Food Sci. Technol.* **2003**, *38*, 445–451.

(18) Mauriello, G.; Moio, L.; Genovese, A.; Ercolini, D. Relationships between flavoring capabilities, bacterial composition, and geographical origin of natural whey cultures used for traditional water buffalo mozzarella cheese manufacture. *J. Dairy Sci.* **2003**, *86*, 486–497.

(19) Ariyama, K.; Aoyama, Y.; Mochizuki, A.; Homura, Y.; Kadokura, M.; Yasui, A. Determination of the geographic origin of onions between three main production areas in Japan and other countries by mineral composition. *J. Agric. Food Chem.* **2007**, *55*, 347–354.

(20) Moreda-Piñeiro, A.; Fisher, A.; Hill, S. J. The classification of tea according to region of origin using pattern recognition techniques and trace metal data. *J. Food Compos. Anal.* **2003**, *16* (2), 195–211.

(21) Boscaini, E.; Van Ruth, S.; Biasioli, F.; Gasperi, F.; Märk, T. D. Gas chromatography−olfactometry (GC-O) and proton transfer reaction-mass spectrometry (PTR-MS) analysis of the favour profile of Grana Padano, Parmigiano Reggiano, and Grana Trentino cheeses. *J. Agric. Food Chem.* **2003**, *51*, 1782–1790.

(22) Luykx, D. M. A. M.; Ruth, S. M. v. An overview of analytical methods for determining the geographical origin of food products. *Food Chem.* **2008**, *107*, 897–911.

(23) Spitaler, R.; Araghipour, N.; Mikoviny, T.; Wisthaler, A.; Via, J. D.; Märk, T. D. PTR-MS in enology: Advances in analytics and data analysis. *Int. J. Mass Spectrom.* **2007**, *266*, 1–7.

(24) Venter, A.; Nefliu, M.; Cooks, R. G. Ambient desorption ionization mass spectrometry. *Trends Anal. Chem.* **2008**, *27* (4), 284–290.

(25) Cooks, R. G.; Ouyang, Z.; Takáts, Z.; Wiseman, J. M. Ambient mass spectrometry. *Science* **2006**, *311*, 1566–1570.

(26) Chen, H. W.; Talaty, N. N.; Takáts, Z.; Cooks, R. G. Desorption electrospray ionization mass spectrometry for high-throughput analysis of pharmaceutical samples in the ambient environment. *Anal. Chem.* **2005**, *77* (21), 6915–6927.

(27) Takáts, Z.; Cotte-Rodríguez, I.; Talaty, N.; Chen, H. W.; Cooks, R. G. Direct, trace level detection of explosives on ambient surfaces by desorption electrospray ionization mass spectrometry. *Chem. Commun.* **2005**, 1950–1952DOI:10.1039/B418697D.

(28) Takaáts, Z.; Wiseman, J. M.; Gologan, B.; Cooks, R. G. Mass spectrometry sampling under ambient conditions with desorption electrospray ionization. *Science* **2004**, *306*, 471–473.

(29) Cotte-Rodríguez, I.; Takáts, Z.; Talaty, N.; Chen, H. W.; Cooks, R. G. Desorption electrospray ionization of explosives on surfaces: Sensitivity and selectivity enhancement by reactive desorption electrospray ionization. *Anal. Chem.* **2005**, *77*, 6755–6764.

(30) Chen, H. W.; Venter, A.; Cooks, R. G. Extractive electrospray ionization for direct analysis of undiluted urine, milk and other complex mixtures without sample preparation. *Chem. Commun.* **2006**, *19*, 2042–2044.

(31) Chen, H. W.; Wortmann, A.; Zhang, W. H.; Zenobi, R. Rapid in vivo fingerprinting of non-volatile compounds in breath by extractive electrospray ionization quadrupole time-of-flight mass spectrometry. *Angew. Chem., Int. Ed.* **2007**, *46* (4), 580–583.

(32) Chen, H. W.; Sun, Y. P.; Wortmann, A.; Gu, H. W.; Zenobi, R. Differentiation of maturity and quality of fruit using non-invasive extractive electrospray ionization quadrupole time-of-flight mass spectrometry. *Anal. Chem.* **2007**, *79* (4), 1447–1455.

(33) Chen, H. W.; Hu, B.; Hu, Y.; Huan, Y. F.; Zhou, Z. Q.; Qiao, X. L. Neutral desorption using a sealed enclosure to sample explosives on human skin for rapid detection by EESI-MS. *J. Am. Soc. Mass Spectrom.* **2009**, *20*, 719–722.

(34) Chen, H. W.; Zenobi, R. Neutral desorption sampling of biological surfaces for rapid chemical characterization by extractive electrospray ionization mass spectrometry. *Nat. Protoc.* **2008**, *3* (9), 1467–1475.

(35) Chen, H. W.; Zheng, J.; Zhang, X.; Lou, M. B.; Wang, Z. C.; Qiao, X. L. Surface desorption atmospheric pressure chemical ionization mass spectrometry for direct ambient sample analysis without toxic chemical contamination. *J. Mass Spectrom.* **2007**, *42*, 1045–1056.

(36) Chen, H. W.; Lai, J. F.; Zhou, Y. F.; Huan, Y. F.; Li, J. Q.; Zhang, X.; Wang, Z. C.; Luo, M. B. Instrumentation and characterization of surface desorption atmospheric pressure chemical ionization mass spectrometry. *Chin. J. Anal. Chem.* **2007**, *35* (8), 1233–1240.

(37) Chen, H. W.; Liang, H. Z.; Ding, J. H.; Lai, J. H.; Huan, Y. F.; Qiao, X. L. Rapid differentiation of tea products by surface desorption atmospheric pressure chemical ionization mass spectrometry. *J. Agric. Food Chem.* **2007**, *55*, 10093–10100.

(38) Yang, S. P.; Ding, J. H.; Zheng, J.; Hu, B.; Li, J. Q.; Chen, H. W.; Zhou, Z. Q.; Qiao, X. L. Detection of melamine in milk products by surface desorption atmospheric pressure chemical ionization mass spectrometry. *Anal. Chem.* **2009**, *81*, 2426–2436.

(39) Andrade, F. J.; Shelley, J. T.; Wetzel, W. C.; Webb, M. R.; Gamez, G.; Ray, S. J.; Hieftje, G. M. Atmospheric pressure chemical ionization source. 2. desorption-ionization for the direct analysis of solid compounds. *Anal. Chem.* **2008**, *80*, 2654–2663.

(40) Jackson, J. E. Principal components and factor analysis:part1-principal components. *J. Qual. Technol.* **1981**, *13* (1), 55–63.
(41) Wold, S. Pattern recognition by means of disjoint principal components models. *Patt. Recognit.* **1976**, *8*, 127–139.
(42) Zhang, X. Q.; Zhou, X.; Wang, D. P.; Hao, X. J. Analysis of alkaloids in *Evodia rutaecarpa* from different habitats by liquid chroamtography/mass spectrometry. *Chin. J. Anal. Chem.* **2005**, *33* (2), 241–244.
(43) Džeroski, S.; Drummb, D. Using regression trees to identify the habitat preference of the sea cucumber (Holothuria leucospilota) on Rarotonga, Cook Islands. *Ecol. Modell.* **2003**, *170*, 219–226.
(44) Foucart, T. Multiple linear regression on canonical correlation variables. *Biom. J.* **1999**, *45* (5), 559–572.
(45) Nefliu, M.; Smith, J. N.; Venter, A.; Cooks, R. G. Internal energy distributions in desorption electrospray ionization (DESI). *J. Am. Soc. Mass Spectrom.* **2008**, *19*, 420–427.
(46) Tuytten, R.; Lemière, F.; Dongen, W. V.; Esmans, E. L. Intriguing mass spectrometric behavior of guanosine under low energy collision induced dissociation: H_2O adduct formation and gas-phase reactions in the collision cell. *J. Am. Soc. Mass Spectrom.* **2005**, *16* (8), 1291–1304.
(47) Sartori, A.; Garay-Malpartida, H.; Forni, M.; Schumacher, R.; Dutra, F.; Sogayar, M.; Bechara, E. Aminoacetone, a putative endogenous source of methylglyoxal, causes oxidative stress and death to insulin-producing RINm5f cells. *Chem. Res. Toxicol.* **2008**, *21* (9), 1841–1850.
(48) Bechara, E.; Dutra, F.; Cardoso, V.; Sartori, A.; Olympio, K.; Penatti, C.; Adhikari, A.; Assuncao, N. The dual face of endogenous α-aminoketones: Pro-oxidizing metabolic weapons. *Comp. Biochem. Physiol., Part C: Toxicol. Pharmacol.* **2007**, *146*, 88–110.
(49) Deng, Y. L.; Yu, P. H. Assessment of the deamination of aminoacetone, an endogenous substrate for semicarbazide-sensitive amine oxidase. *Anal. Biochem.* **1999**, *270* (1), 97–102.
(50) Hiraku, Y.; Sugimoto, J.; Yamaguchi, T.; Kawanishi, S. Oxidative DNA damage induced by aminoacetone, an amino acid metabolite. *Arch. Biochem. Biophys.* **1999**, *365* (1), 62–70.
(51) Lyles, G.; Chalmers, J. The metabolism of aminoacetone to methylglyoxal by semicarbazide-sensitive amine oxidase in human umbilical artery. *Biochem. Pharmacol.* **1992**, *43* (7), 1409–1414.
(52) Flaten, G. R.; Grung, B.; Kvalheim, O. M. A method for validation of reference sets in SIMCA modelling. *Chemom. Intell. Lab. Syst.* **2004**, *72*, 101–109.
(53) Kubicka, D.; Rönnholm, M.; Reinikainen, S. P.; Salmi, T.; Murzin, D. Y. Improved kinetic data from analysis of complex hydrocarbon mixtures by using SIMCA. *Anal. Chim. Acta* **2005**, *537*, 339–348.

Received January 8, 2009. Revised manuscript received September 4, 2009. Accepted September 7, 2009.